NASA TECHNICAL
MEMORANDUM

NASA TM X-64963

A TETHER TENSION CONTROL LAW FOR TETHERED SUBSATELLITES DEPLOYED ALONG LOCAL VERTICAL

By Charles C. Rupp

Preliminary Design Office
Program Development

NASA

George C. Marshall Space Flight Center
Marshall Space Flight Center, Alabama

1. REPORT NO. NASA TM X-64963	2. GOVERNMENT ACCESSION NO.	3. RECIPIENT'S CATALOG NO.
4. TITLE AND SUBTITLE A Tether Tension Control Law for Tethered Subsatellites Deployed Along Local Vertical		5. REPORT DATE September 1, 1975
		6. PERFORMING ORGANIZATION CODE
7. AUTHOR(S) Charles C. Rupp		8. PERFORMING ORGANIZATION REPORT #
9. PERFORMING ORGANIZATION NAME AND ADDRESS George C. Marshall Space Flight Center Marshall Space Flight Center, Alabama 35812		10. WORK UNIT NO.
		11. CONTRACT OR GRANT NO.
12. SPONSORING AGENCY NAME AND ADDRESS National Aeronautics and Space Administration Washington, D.C. 20546		13. TYPE OF REPORT & PERIOD COVERED Technical Memorandum
		14. SPONSORING AGENCY CODE

15. SUPPLEMENTARY NOTES

Prepared by Preliminary Design Office, Program Development

16. ABSTRACT

A tethered subsatellite deployed along the local vertical is in stable equilibrium. This applies equally to subsatellites deployed in the direction towards the earth from the main spacecraft or away from the Earth. Momentary perturbations from this stable equilibrium will result in a swinging motion, which decays very slowly if passive means are relied upon to provide damping. A control law is described which actively damps the swinging motion by commanding a reel, or other mechanism, to apply appropriate tension as a function of tetherline length, rate of change of length, and desired length. The same control law is shown to be useful for deployment and retrieval of tethered subsatellites in addition to damping to steady state.

17. KEY WORDS		18. DISTRIBUTION STATEMENT	
19. SECURITY CLASSIF. (of this report) Unclassified	20. SECURITY CLASSIF. (of this page) Unclassified	21. NO. OF PAGES 31	22. PRICE NTIS

TABLE OF CONTENTS

LIST OF ILLUSTRATIONS

A TETHER TENSION CONTROL LAW FOR TETHERED SUBSATELLITES DEPLOYED ALONG LOCAL VERTICAL

SECTION I. INTRODUCTION

A. Historical Development of Tetherline

The use of tethers has been proposed in the past for a multitude of purposes. One significant study effort was directed towards the retrieval of stranded astronauts by using tetherlines [1, 2, 3]. The approach was to "throw a buoy" from a rescue vehicle towards an astronaut. The buoy would be attached to the astronaut and then reeled in.

Reference 1 contains a derivation of relative motion equations. Also included are nomographs which enable one to determine the initial ejection velocity relative to the main spacecraft and the constant tether tension required to cause the trajectory to pass through the desired point. The scheme, as presented, is open loop; that is, there is no control over perturbations from the desired trajectory.

The significant contribution of reference 2 was a description of the problems associated with retrieval, especially the terminal phase, when relative velocities and angular rates can become quite large. Here again, the control was open loop, thus small perturbations in the system at the beginning of the retrieval can cause large deviations at the terminal phase.

Reference 3 presented a concept for a reel mechanism for controlling line tension and a "fish pole" to aid in preventing tangling. Rather stringent tolerances were required to assure that the control system could control the trajectory as desired. A closed loop scheme was implied, but the control law was not discussed.

Another body of work was directed towards station keeping requirements. Reference 4 describes a scheme designed to tether a modified lunar module and Apollo telescope mount (LM-ATM) to an orbital workshop (OWS). This scheme

required periodic tugs on the tetherline to cause the LM-ATM to move about the OWS. A repetitive, somewhat egg shaped trajectory relative to the OWS could be obtained by accurately timing and metering tether tension during the tugging operation. The scheme presented safety hazards and required constant attention by the crew and was judged to be an unattractive flight configuration.

Manned flight experience with tethers was obtained on Gemini XI and XII. Reference 5 describes these experiences. The Gemini XI flight demonstrated a rotating configuration with the Gemini spacecraft tied to an Agena by 100 ft of dacron webbing and spinning at 0.9 deg/s. The Gemini XII flight demonstrated gravity gradient capture. Insertion into the stable equilibrium was difficult because of thruster failures, but peak amplitudes of less than 60 deg from local vertical were observed.

The Radio Astronomy Explorer (RAE) flight experience is of interest [6]. The RAE uses a combination of magnetic torquing, long (750 ft) booms, and hysteresis damping to bring the vehicle close to steady state equilibrium. To achieve rapid damping, the booms were deployed at opportune times in the spacecraft attitude oscillation. The effect was to decrease the attitude rate by increasing the inertia of the spacecraft. Subsequent deployment of a hysteresis damper rapidly reduced libration amplitudes to steady state. Although this experience does not involve tethers, the rather long booms exhibit some of the same characteristics of tetherlines and some of the same techniques can be used to damp tetherline motion.

B. Objectives of This Study

All of the previously mentioned projects, with the exception of the RAE and Gemini XII flight, involve the use of tetherlines (or long booms) in dynamic modes of operation. The objective of this study, however, is to design a control law which will cause the motions (swinging and stretching) of a tetherline to be damped to the steady state equilibrium. It will be shown that structural damping in the tetherline will cause motion of a tethered subsatellite to be damped. Normally, this damping is nearly inconsequential, but an active system will be shown which enhances the damping to the point where even large amplitude oscillations in the orbital plane can be damped to nearly zero in two cycles.

The equations of motion presented are planar to simplify the presentation, but the control law has been studied in a three degree-of-freedom relative motion orbital simulation. The effects of atmospheric drag have been lumped at the subsatellite and the tetherline is assumed to be massless.

2

SECTION II. EQUATIONS OF MOTION

Figure 1 portrays a small subsatellite tethered to the main satellite, in this case the orbiter. It is assumed that the orbiter mass is much larger than that of the subsatellite and the orbit is circular so the orbit rate, $\dot{\phi}$, is constant. From reference 1 the equations of motion for the subsatellite relative to the main body, considering motion only in the orbital plane and a massless tetherline, are:

$$\ddot{\ell} = \ell(\dot{\phi} + \dot{\theta})^2 + \dot{\phi}^2 r_1 \left[(1 - \Delta^{-3}) \cos \theta - \frac{\Delta^{-3} \ell}{r_1} \right] - H \frac{\tau}{M_2} \tag{1a}$$

$$\ddot{\theta} = -\frac{2 \dot{\ell}(\dot{\phi} + \dot{\theta})}{\ell} - \frac{\dot{\phi}^2 r_1 (1 - \Delta^{-3}) \sin \theta}{\ell} \tag{1b}$$

$$\Delta^{-3} = \left(1 + 2 \frac{\ell}{r_1} \cos \theta + \frac{\ell^2}{r_1^2} \right)^{-3/2} \tag{1c}$$

$$\tau = K(\ell - \ell_0) + c\dot{\ell} \tag{1d}$$

where

c = tetherline coefficient of viscous damping

K = tetherline spring constant

ℓ_0 = unstretched tetherline length

H = operator whose value is 1 if $\ell \geq \ell_0$, 0 if $\ell < \ell_0$

r_1 = radius of the orbiter orbit

τ = tether tension   .

3

Equation (1a) is referred to as the length equation and (1b) as the swing equation. Inspection of equation (1b) shows that $\theta = 0$, π are equilibrium solutions; that is, $\ddot{\theta} = 0$ when $\dot{\ell} = \dot{\theta} = 0$ and $\theta = 0$ or π. At the equilibrium solution:

$$\theta = 0 \, , \, \Delta^{-3} = 1 - 3\frac{\ell}{r_1} + 6\left(\frac{\ell}{r_1}\right)^2 - 10\left(\frac{\ell}{r_1}\right)^3 \ldots \tag{2a}$$

$$\theta = \pi \, , \, \Delta^{-3} = 1 + 3\frac{\ell}{r_1} + 6\left(\frac{\ell}{r_1}\right)^2 + 10\left(\frac{\ell}{r_1}\right)^3 \ldots \tag{2b}$$

Setting $\dot{\theta} = 0$ and taking the first 2 terms for Δ^{-3} in equation (1a) gives:

for $\theta = 0$,

$$\ddot{\ell} = \ell(\dot{\phi})^2 + \dot{\phi}^2 r_1\left[2\frac{\ell}{r_1} + 3\left(\frac{\ell}{r_1}\right)^2\right] - H\left[\frac{K}{M_2}(\ell - \ell_0) + \frac{C}{M_2}\dot{\ell}\right] \tag{3a}$$

for $\theta = \pi$,

$$\ddot{\ell} = \ell(\dot{\phi})^2 + \dot{\phi}^2 r_1\left[2\frac{\ell}{r_1} - 3\left(\frac{\ell}{r_1}\right)^2\right] - H\left[\frac{K}{M_2}(\ell - \ell_0) + \frac{C}{M_2}\dot{\ell}\right] . \tag{3b}$$

Dropping the $\left(\frac{\ell}{r_1}\right)^2$ term and assuming positive tension reduces equation (3) to a linear differential equation:

$$\ddot{\ell} = -\frac{C}{M_2}\dot{\ell} - \left(\frac{K}{M_2} - 3\dot{\phi}^2\right)\ell + \frac{K}{M_2}\ell_0 \quad . \tag{4}$$

The parameters for damping ratio, ξ, and natural frequency, ω_n, for the stretch equation are:

4

$$\omega_n = \sqrt{\frac{K}{M_2} - 3\dot{\phi}^2} \qquad\qquad (5a)$$

$$\xi = \frac{C}{2\,M_2\,\omega_n} \qquad . \qquad\qquad (5b)$$

Note that the usual natural frequency of a spring mass system is modified by a gravity gradient term, $3\dot{\phi}^2$. This implies that the spring constant term, K/M_2, must be larger than the gravity term if steady state equilibrium is to exist. The final value of ℓ is given by

$$\ell_{ss} = \frac{\dfrac{K}{M_2}\,\ell_o}{\dfrac{K}{M_2} - 3\dot{\phi}^2} \qquad . \qquad\qquad (6)$$

Equation (6) neglects higher order terms due to gravity gradient. An error of approximately 2% exists in the stretch due to this omission which is acceptable for most analyses.

The natural frequency and damping ratio of the swing equation, (1b), can be approximated in a similar fashion assuming constant $\dot{\ell}$. For θ close to 0 or π, equation (1b) is approximated by

$$\ddot{\theta} = -2\frac{\dot{\ell}}{\ell}\dot{\theta} - 3\dot{\phi}^2\theta - 2\frac{\dot{\ell}}{\ell}\dot{\phi} \qquad . \qquad\qquad (7)$$

The damping ratio and natural frequency are

$$\omega_n = \sqrt{3}\,\dot{\phi} \qquad\qquad (8a)$$

$$\xi = \frac{\dot{\ell}}{\ell\omega_n} \qquad . \qquad\qquad (8b)$$

Inspection shows that the swinging frequency is independent of ℓ and that the swinging motion is damped during deployment where $\dot{\ell} > 0$. The damping can be significant as can be seen from an illustration. Consider a deployment rate of 5 m/s, a length of 10 km, and $\dot{\phi} = 0.00\ 1185$ rad/s. The damping ratio is 0.24.

Maintenance of a fixed length or retraction of a tetherline causes the damping term to disappear or change polarity (indicating instability). Additional means of control must be employed to enable satisfactory performance for the latter two operations.

SECTION III. DEVELOPMENT OF A TETHER CONTROL LAW

Quite often, a system which has coupling from one mode of vibration to another can be stabilized by adding damping to one mode only. The effectiveness of this procedure depends, among other things, on the degree of coupling between the modes. In the case of the tethered subsatellite, viscous damping in the tetherline aids in damping the swinging motion. The viscous damping of materials which could be used for tetherlines is very low. However, a tether reel located in the orbiter can be controlled in a manner which simulates any damping or spring constant. Implementation of such a control law requires sensing tether tension, rate of line deployment, and length of line deployed. A computer calculates the tension as a function of the rate and line length required to simulate a spring with the desired characteristics. The computer then commands the reel motor to produce the required tension. The tension at the subsatellite end of the tetherline approximates the tension at the orbiter end if the tether mass is negligible. If not negligible, the mass of the line causes delay and change of amplitude of tension which can be predicted and compensated by the computer.

Computer simulation results will now be shown which illustrate the damping of initial conditions for natural damping obtained from tetherline materials and controlled damping obtained from a reel mechanism control law. Consider a tetherline system with the following characteristics:

$\dot{\phi}$ = 0.001185 rad/s

K = 0.2 N/m

6

$$M_2 = 100 \text{ kg}$$

$$C = 0.1 \text{ N-s}^2/\text{m}$$

$$l_o = 4 \text{ km} \quad .$$

A trajectory of this system in a rotating local vertical coordinate frame is shown in Figure 2. The subsatellite is initia' :ed at 4 km which is approximately the unstretched tetherline length. The tether tension was zero whenever the length was less than approximately 4005 m as indicated by the dotted trajectory. Length increases positively in a downward direction. A small amount of damping is evident due mainly to structural damping which is 1.1% of critical damping. Figure 3 shows a plot of the swing angle, θ, versus time and negligible damping of the swinging motion can be observed.

From the preceding example, additional control is required if initial conditions are to be damped. It is evident that little coupling exists from the swinging motion to the stretching motion. This is due in part to the wide difference in the resonant frequencies of the two vibrations as seen by comparing equation (5a) to equation (8a). Equation (8a) shows that the swing frequency is a function of only the orbital rate and no adjustment is possible, but equation (5a) includes the spring constant, K, and mass of the subsatellite which can be adjusted. For a given subsatellite mass, the tetherline spring constant can be selected to yield a wide range of stretch natural frequencies. The tetherline material can be selected to give the desired spring constant or it is much preferred to design a reel mechanism control law to give an effective spring constant as required. The effective spring constant programmed into the reel mechanism controller is in series with that of the tetherline, and the tetherline spring constant can be made negligible compared to that of the reel mechanism. Since it is desired to make the stretch frequency equal to the swing frequency, the required spring constant can be found by equating equations (5a) and (8a) and solving for K_1:

$$K_1 = 6\dot{\phi}^2 M_2 \quad . \tag{9}$$

Similarly, an effective coefficient of viscous damping can be programmed into the reel mechanism. Equation (5b) can be used to determine the coefficient required for a given damping ratio:

7

$$C_1 = 2 M_2 \sqrt{\frac{K_1}{M_2} - 3\dot{\phi}^2}\ \xi \qquad . \tag{10}$$

The reel mechanism control law used has essentially the same form as equation (1d):

$$\tau = K_1 \ell + C_1 \dot{\ell} + K_2 \ell_c \qquad . \tag{11}$$

Instead of ℓ_0, which is the initial unstretched length of the tetherline, ℓ_c denotes the commanded length. The factor K_2 is found from an equation similar to equation (4):

$$\ddot{\ell} = -\frac{C_1}{M_2}\dot{\ell} - \left(\frac{K_1}{M_2} - 3\dot{\phi}^2\right)\ell + \frac{K_2}{M_2}\ell_c \qquad . \tag{12}$$

The steady state solution of (12) is

$$\left(\frac{K_1}{M_2} - 3\dot{\phi}^2\right)\ell = \frac{K_2}{M_2}\ell_c \qquad . \tag{13}$$

Forcing $\ell = \ell_c$ gives the value required for K_2:

$$K_2 = M_2 \left(\frac{K_1}{M_2} - 3\dot{\phi}^2\right) \qquad . \tag{14}$$

The control law, equation (11), commands tetherline tension as a function of amount of line played out, rate of line deployment or retrieval and commanded length. Thus, three sensors are required to implement the control law.

The effectiveness of the control law can be demonstrated using the following characteristics:

8

$$M_2 = 100 \text{ kg}$$

$$\ell_c = 4100 \text{ m}$$

$$\ell_o = \text{initial value of } \ell = 4000 \text{ m}$$

$$\xi = 1.0$$

$$\dot{\phi} = 0.001185 \text{ rad/s} \quad.$$

Using equation (9), $K_1 = 8.43$ E-4 N/m; using equation (10), $C_1 = 0.410$ N-s/m; and using equation (14), $K_2 = 4.22$ E-4 N/m. A tetherline system with this control law has a trajectory as shown in Figure 4. The swing angle as a function of time is shown in Figure 5. This demonstrates the greatly improved results obtainable by controlling the tetherline.

SECTION IV. DEPLOYMENT OF TETHERLINES

One of the applications of tetherlines required deployment of tetherlines 100 km long [7]. The quickest way to show the feasibility of deploying such long tetherlines is to use the control law developed in Section III. The sub-satellite could be given an initial ejection velocity and the commanded length in the control law could be adjusted as required to obtain ᵃn acceptable trajectory.

A problem arose which caused the subsatellite to free-fly. If the commanded length is too large compared to the present length and velocity, the tension commanded by the control law is negative which is an impossible operation to perform on a flexible tetherline. An immediate fix was applied which consisted of incrementing the commanded length. Table 1 gives the commanded length and increments to achieve a deployment of 100 km. The resulting trajectory is shown in Figure 6. Plots of tether acceleration and deployment rate are shown in Figures 7 and 8, respectively.

One can envision other control laws which could effect the deployment in a more optimal fashion, eliminating the jerky deployment rates when the commanded length is changed. This job, left for future investigations, is beyond the scope of this preliminary feasibility study.

9

TABLE 1. DEPLOYMENT SEQUENCE

- Aerodynamic drag is neglected

- ℓ_c neglects drag and higher order gravity gradient terms

- Initial conditions: $\ell_o = 1$ m, $\dot{\ell}_o = 0.5$ m/s, $\theta_o = 180°$, $\dot{\theta}_o = 0$

- Subsatellite is lowered in steps by changing ℓ_c at times indicated

Time (hr)	0	0.74	1.47	2.18	2.90	3.61	4.32	5.03
ℓ_c (km)	0.42	0.74	1.29	2.26	3.95	6.92	12.1	21.2

Time (hr)	5.75	6.46	7.78	7.89	8.60	9.31	10.02	10.73
ℓ_c (km)	30	40	50	6C	70	80	90	100

Note: The times given are the times at which θ was observed to pass through 180 deg in a positive direction.

SECTION V. RETRIEVAL OF TETHERLINES

The concluding remarks of Section II pointed out the negative damping of the swinging motion which results when tetherlines are retrieved. This problem can be overcome by at least two approaches. One possible solution is to accomplish the retrieval in steps, letting the control law damp the motion between the steps. Another scheme is to retrieve the subsatellite slow enough so that the positive damping in the control law is still sufficient to overcome the negative damping in the swing equation. The latter scheme might be more sensitive to initial conditions than the former, but should be less time consuming.

An example of the first approach is shown in Figure 9. The trajectory shown is the result of commanding the control law to retrieve the tetherline to 50 km in length from an initial 100 km. Damping of the swinging motion induced is accomplished in approximately 1-1/2 hours.

10

An example of the second scheme was not performed. Again, the study was limited to a determination of feasibility, so only one promising approach was pursued.

SECTION VI. INCLUSION OF AERODYNAMICS

The very long tetherline application proposed by reference 7 involved operation at altitudes of 90-120 km where aerodynamic drag can not be neglected. Accordingly, the equations in Section II were modified to include the effects of aerodynamic drag on the subsatellite and the tetherline itself. It is felt that a good approximation is to lump the total drag of the entire tetherline system at the subsatellite.

Figure 10 depicts the aerodynamic model of the tetherline system. If the tetherline is along local vertical so that $\theta = \pi$, the altitude of the sub-satellite, A_s, is

$$A_s = A_o - \ell \quad , \tag{15}$$

where A_o is the altitude of the orbiter and ℓ is tetherline length. The drag on an incremental length of tetherline is given by

$$\Delta F_d = \frac{1}{2} \rho V^2 C_D D \Delta \ell \quad , \tag{16}$$

where

ρ = atmospheric density at the altitude of the segment

V = velocity of the tetherline segment relative to the atmosphere

C_D = drag coefficient of the tetherline

D = diameter of the tetherline

$\Delta \ell$ = length of the segment of tetherline.

11

Figure 11 presents a plot of the drag exerted on each kilometer of a typical tetherline along local vertical using data from the U.S. Standard Atmosphere, 1962. The plot shows that the lower few kilometers of tetherline is where the majority of the drag is concentrated. This phenomenon justifies the assumption that the total system drag can be lumped at the subsatellite.

The density, ρ, varies with the altitude (or length) so the total drag on the tetherline must be found by integrating equation (16):

$$F_d = \frac{1}{2} V^2 C_D D \int_{\ell=0}^{\ell=A_s} \rho \, d\ell \quad . \tag{17}$$

Since the tetherline is generally not along local vertical ($\theta \neq \pi$), the altitude of the subsatellite, A_s, can be approximated given ℓ, θ, and A_o:

$$A_s \approx A_o - \ell \cos(\theta - \pi) \quad . \tag{18}$$

Another consequence of $\theta \neq \pi$ is that the cross sectional area of the tetherline presented to the atmospheric drag is reduced by $\cos(\theta - \pi)$. Equation (17) becomes

$$F_d = \frac{1}{2} V^2 C_D D \int_{\ell=0}^{\ell=A_o - \ell \cos(\theta - \pi)} \rho \cos(\theta - \pi) \, d\ell \quad . \tag{19}$$

A very good exponential curve fit can be found for the drag force which eliminates the need to evaluate the integral in equation (19). Assuming the orbiter is at 200 km and A_s is given in km,

$$\int_{\ell=0}^{\ell=A_o \ell \cos(\theta-\pi)} \rho \cos(\theta - \pi) \, d\ell \approx 10^3 \, EXP \left(18.057 - 0.45602 \, A_s + 0.001495 \, A_s^2\right) .$$

$$\tag{20}$$

The above curve fit is suitable for subsatellite altitudes ranging from 150 km down to 80 km. For higher altitudes, the aerodynamic drag is negligible so the drag force F_d is set to zero.

The acceleration of the subsatellite caused by the drag force is given by

$$\ddot{X}_d = \frac{F_d}{M_s + M_t} \quad , \tag{21}$$

where M_s is the subsatellite mass and M_t is the mass of the tetherline. The total drag acceleration can be divided into two components:

$$\ddot{\ell}_d = -\ddot{X}_d \sin \theta \tag{22}$$

$$\ddot{T}_d = -\ddot{X}_d \cos \theta \quad , \tag{23}$$

where $\ddot{\ell}_d$ is directed along the tetherline and $\ddot{T}_d$ is perpendicular to the tetherline. The angular acceleration with respect to the rotating frame caused by $\ddot{T}_d$ is

$$\ddot{\theta}_d = \frac{\ddot{T}_d}{\ell} \quad . \tag{24}$$

These accelerations caused by aerodynamic drag can now be added to equations (1a) and (1b):

$$\ddot{\ell} = \ell(\dot{\phi} + \dot{\theta})^2 + \dot{\phi}^2 r_1 \left[(1 - \Delta^{-3}) \cos \theta - \frac{\Delta^{-3} \ell}{r_1} \right] - \bar{H} \frac{\tau}{M_2} + \ddot{\ell}_d \tag{25a}$$

$$\ddot{\theta} = -2 \frac{\dot{\ell}}{\ell} (\dot{\phi} + \dot{\theta}) - \dot{\phi}^2 \frac{r_1}{\ell} (1 - \Delta^{-3}) \sin \theta + \ddot{\theta} \, d \quad . \tag{25b}$$

13

An example has been simulated using the following parameters:

A_o = 200 km $\qquad$ $\dot{\phi}$ = 0.001185

V = 7304 m/s $\qquad$ r_1 = 6571 km

C_D = 2.2 $\qquad$ K_1 = 1.651 E-3

$\qquad\qquad\qquad\qquad$ K_2 = 9.436 E-4

M_s = 168 kg $\qquad$ C_1 = 3.98

M_t = 24 kg $\qquad$ D = 3.66×10^{-3} m

The initial conditions for this case are:

$\dot{l}$ = 0 , l = 70 km , l_c = 80 km

$\dot{\theta}$ = 0 , θ = π .

At intervals of 2650 s, the value of l_c was increased by 10 km to a final value of 110 km. The trajectory of this simulation is shown in Figure 12.

SECTION VII. CONCLUSIONS AND RECOMMENDATIONS

The deployment of long tetherlines (100 km) has been shown to be promising from a mechanics viewpoint, but several mechanics and dynamics questions remain open. The out-c. plane motion was not analyzed in this study, and only a few simulations of the de. yment of tetherlines were made on a three degree-of-freedom relative motion simulation [8]. The results of these few simulations demonstrated that out-of-plane motion was bounded during deployment and steady state operation with more out-of-plane motion occurring in simulations of polar orbits than for 28.5 deg inclined orbits. The out-of-plane motion for inclined orbits was excited by out-of-plane components of the relative wind caused by the rotating atmosphere.

Damping of inplane motion excited during tetherline retrieval was simulated, but it is expected that damping of out-of-plane motion will be difficult. The analysis should be extended to include out-of-plane motion so that suitable techniques can be studied for control.

14

Additionally, a modal analysis should be performed on a distributed mass model of the tetherline. This work is required to verify that tetherline dynamics is not a problem.

These comments are relative to the feasibility of tethered subsatellites from a mechanics viewpoint. Additional work also needs to be done in the areas of thermodynamics, materials, orbiter interaction, communication, tracking, subsatellite design, experiment accommodation, etc. It is hoped that the analysis and design of the control law presented in this report are a contribution to the tethered subsatellite technology.
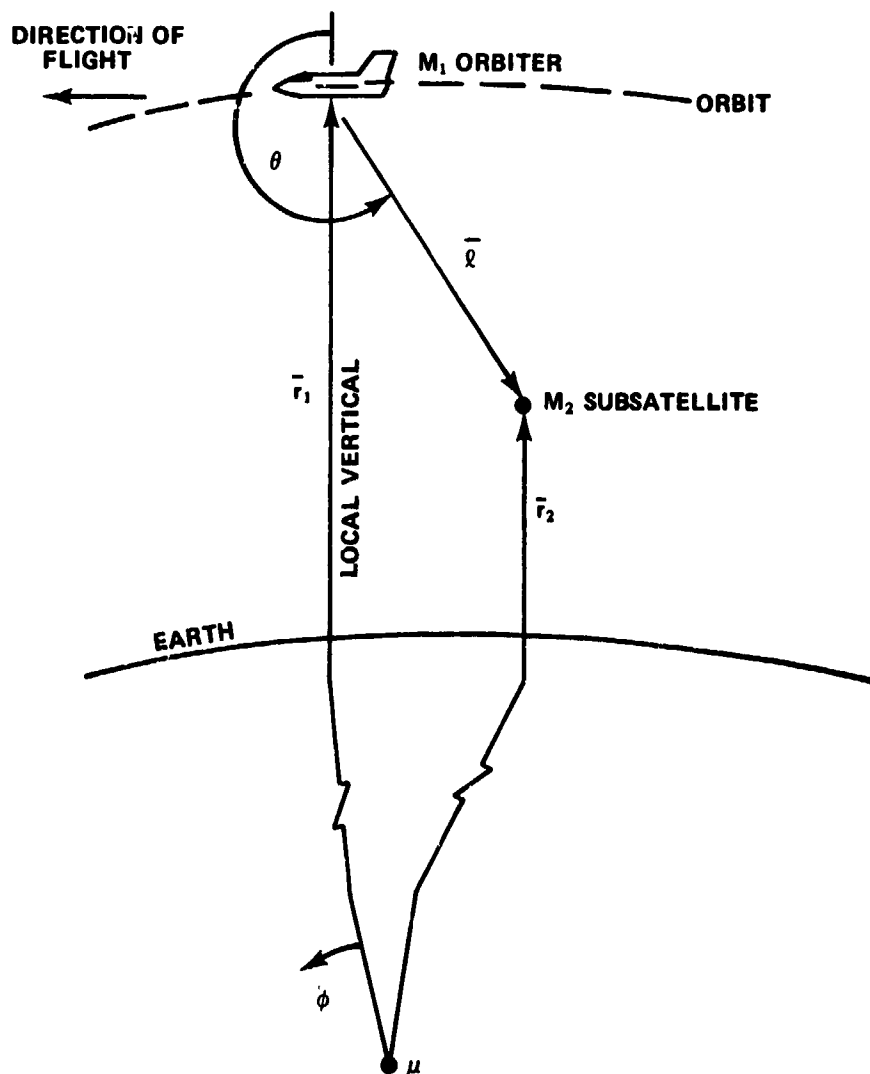
Figure 1. Small subsatellite tethered to the main satellite.
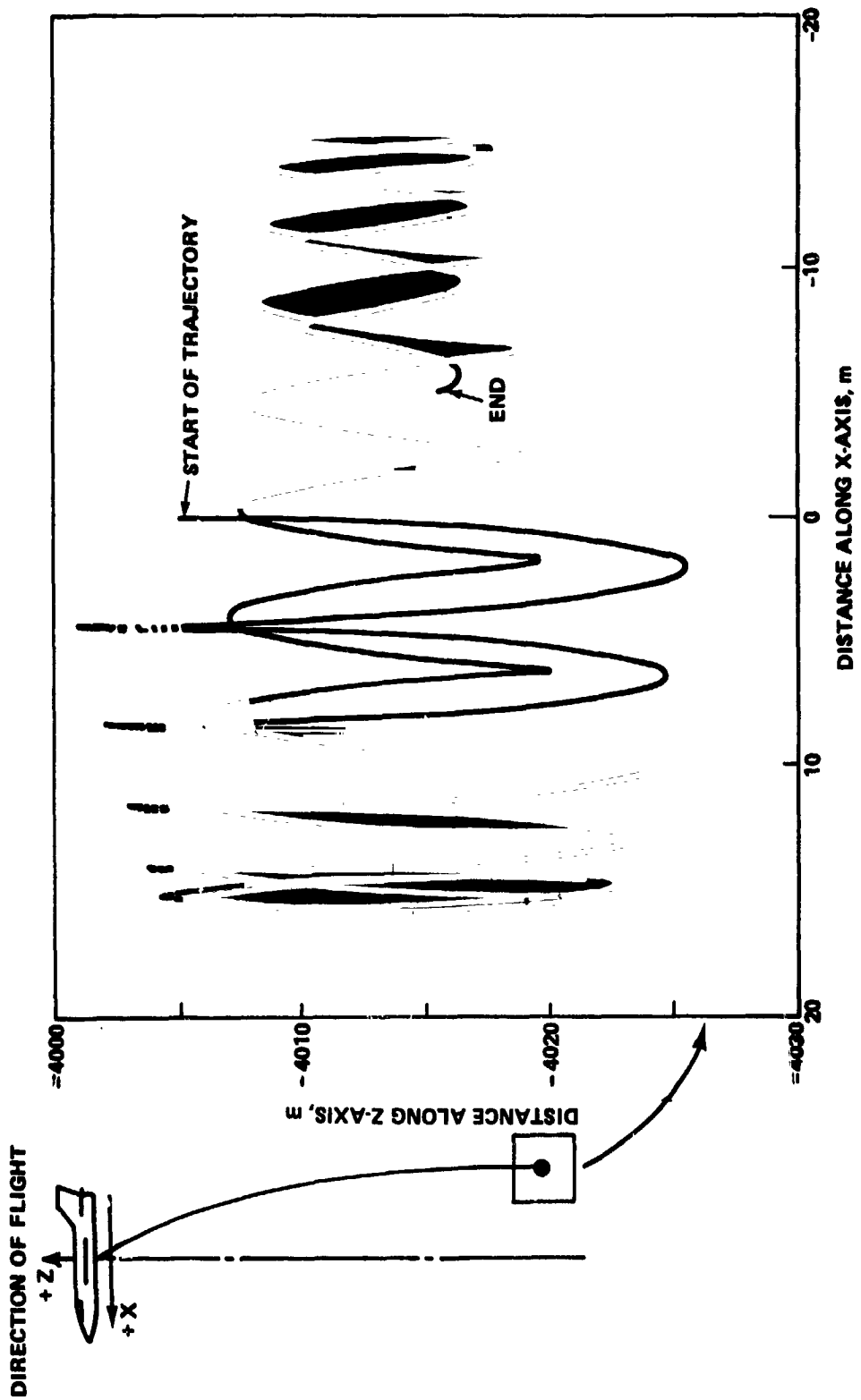
Figure 2. Trajectory of tethered subsatellite with no active control.
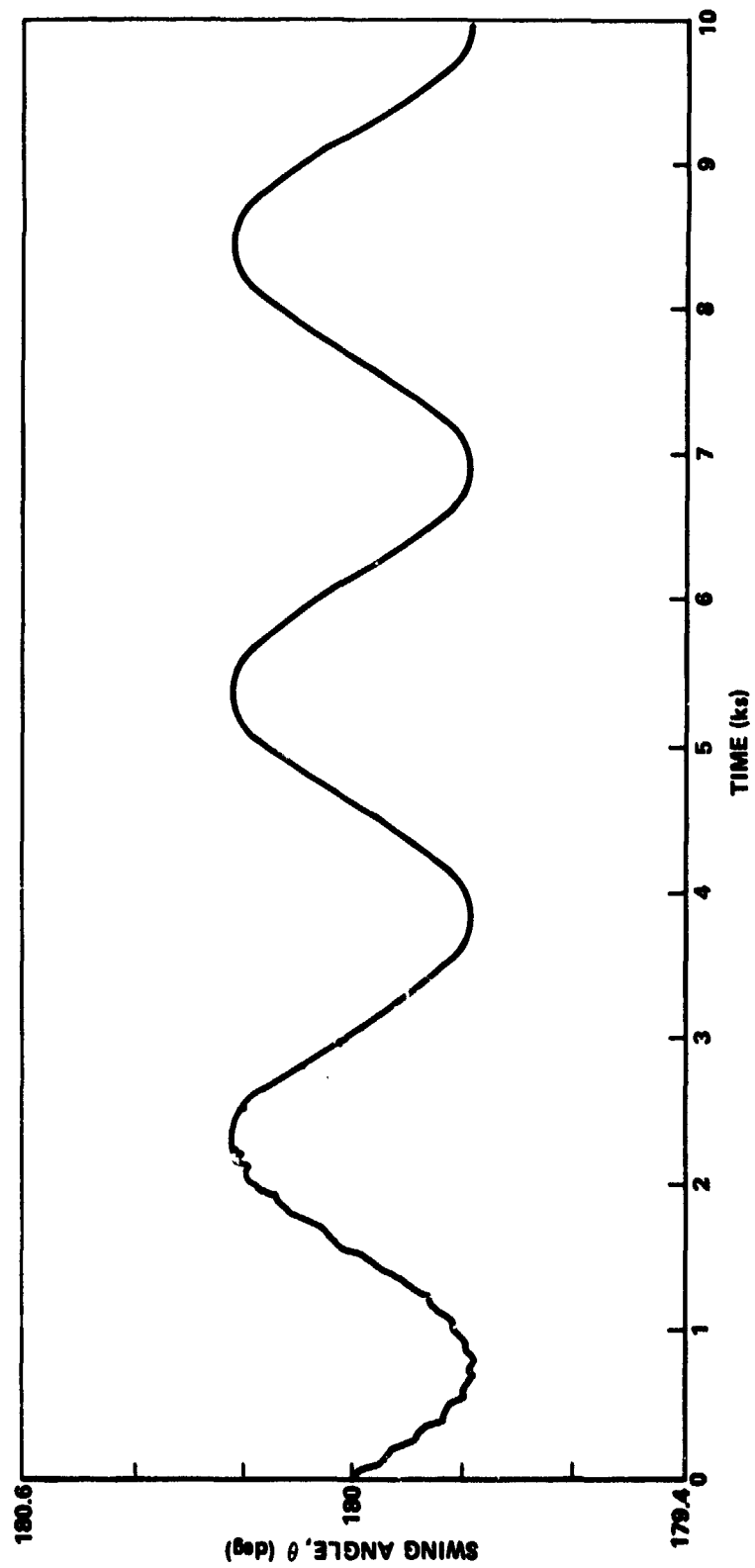
Figure 3. Swing angle, θ, as a function of time for a tether system with no active control.
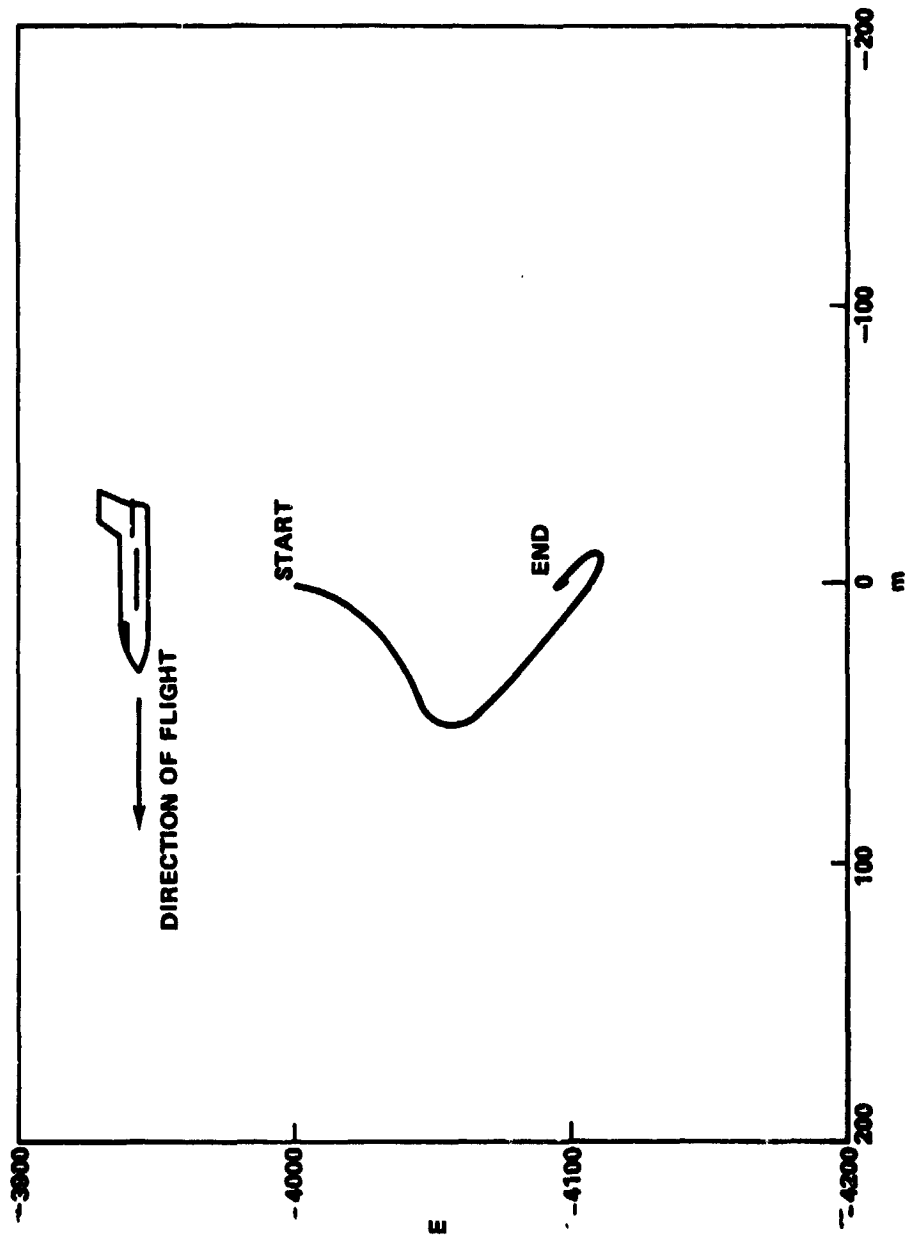
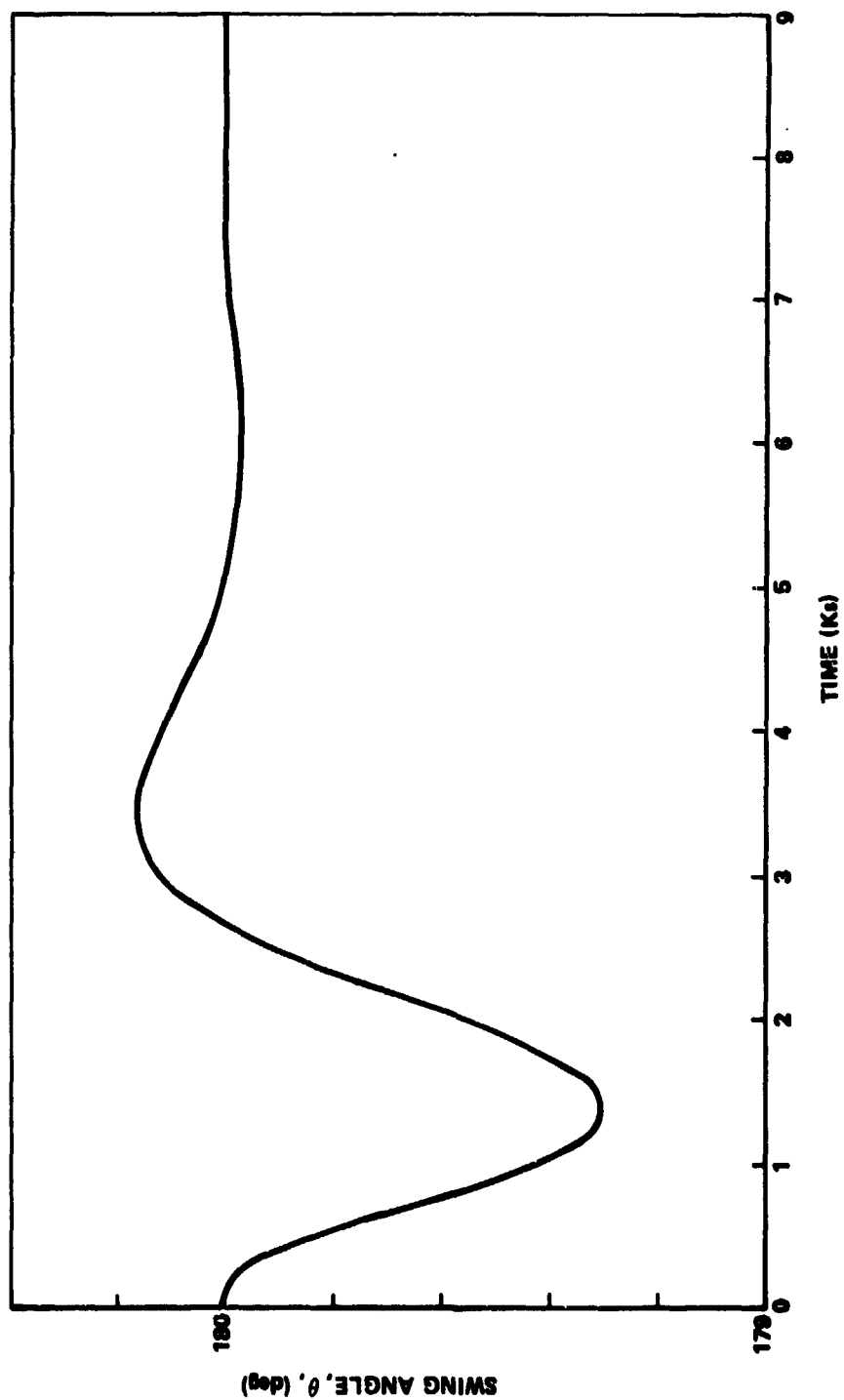Figure 4. Trajectory of tethered subsatellite with active control.

18

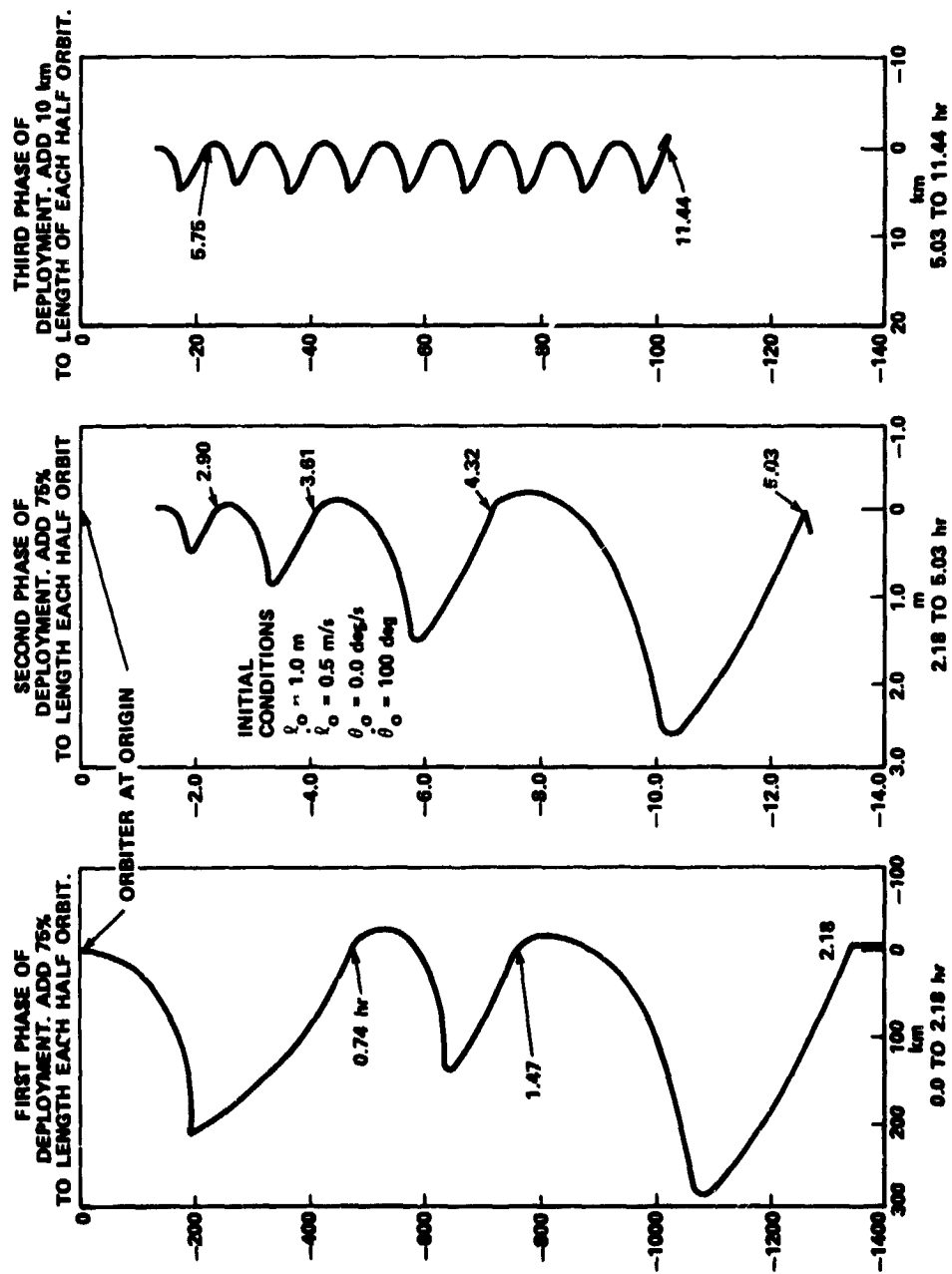Figure 5. Swing angle, θ, as a function of time for a tether system with active control.
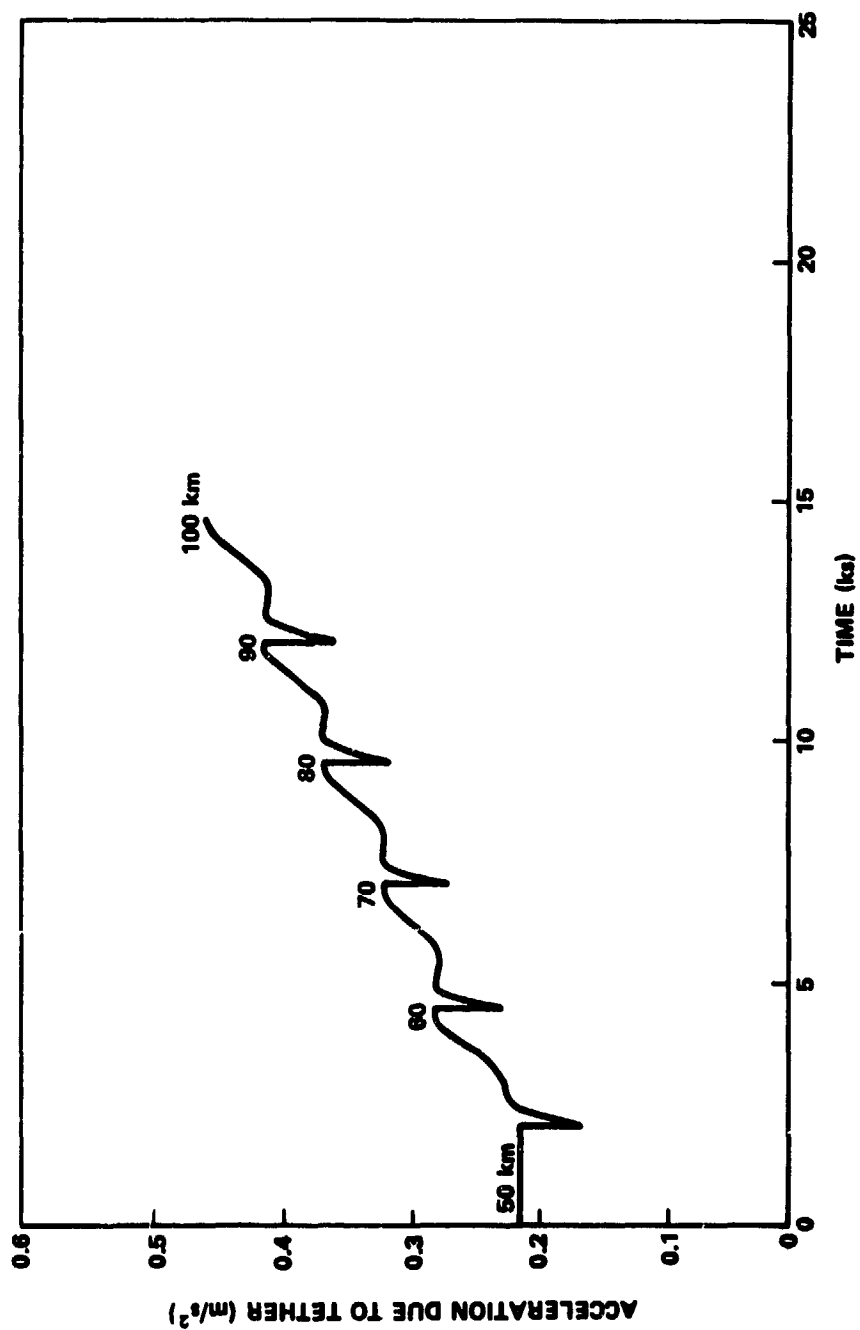
19

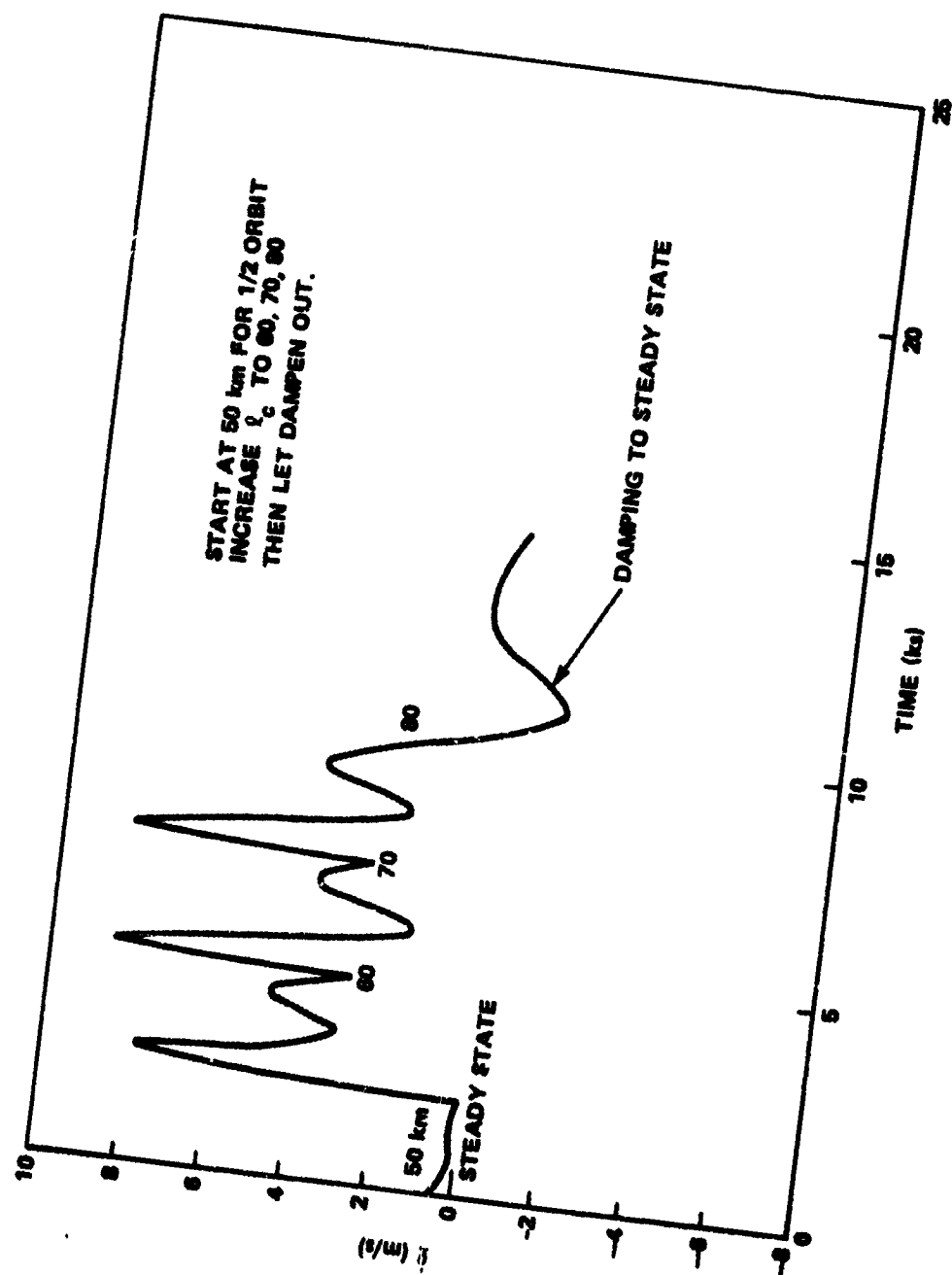Figure 6. Deployment Trajectory.

20

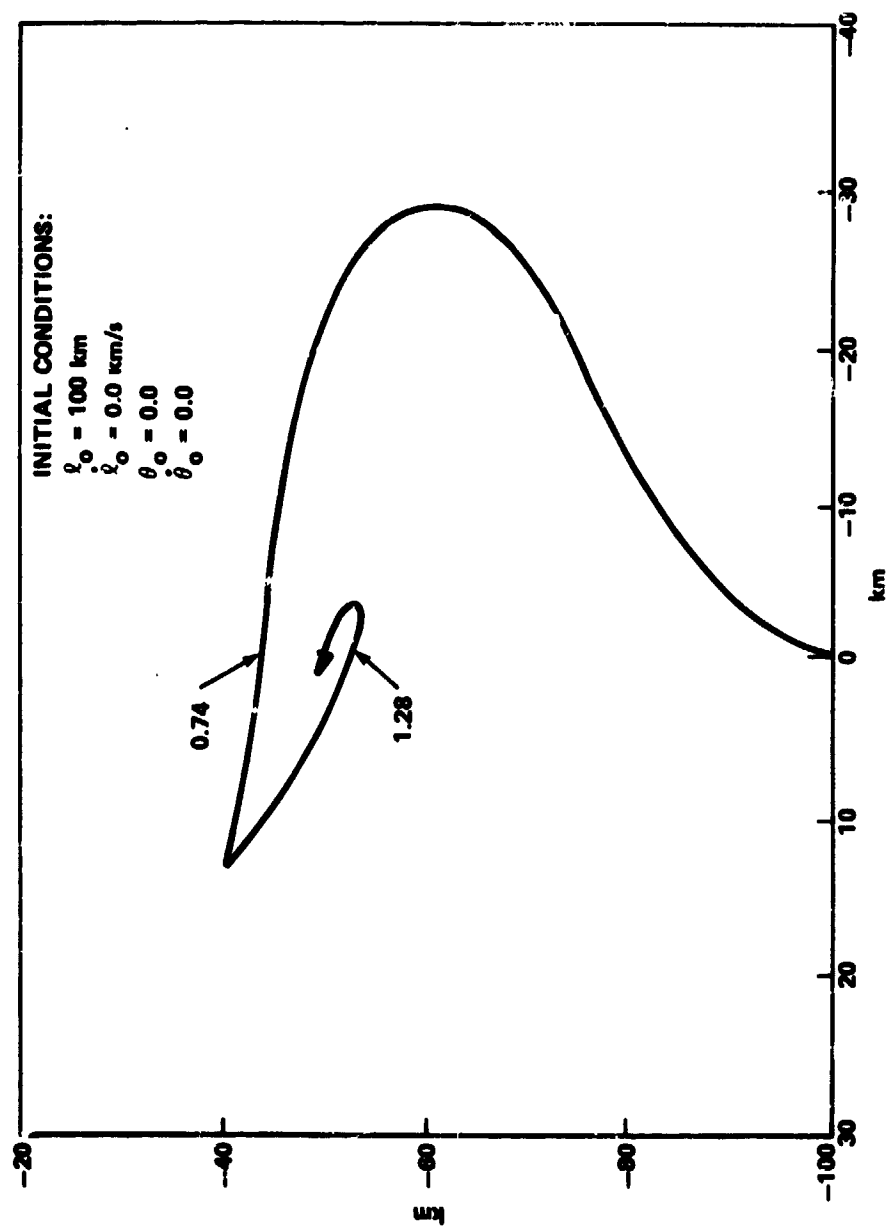Figure 7. Tether acceleration.

21

Figure 8. Deployment rate.

22

INITIAL CONDITIONS:

ℓ_o = 100 km
$\dot{\ell}_o$ = 0.0 km/s
θ_o = 0.0
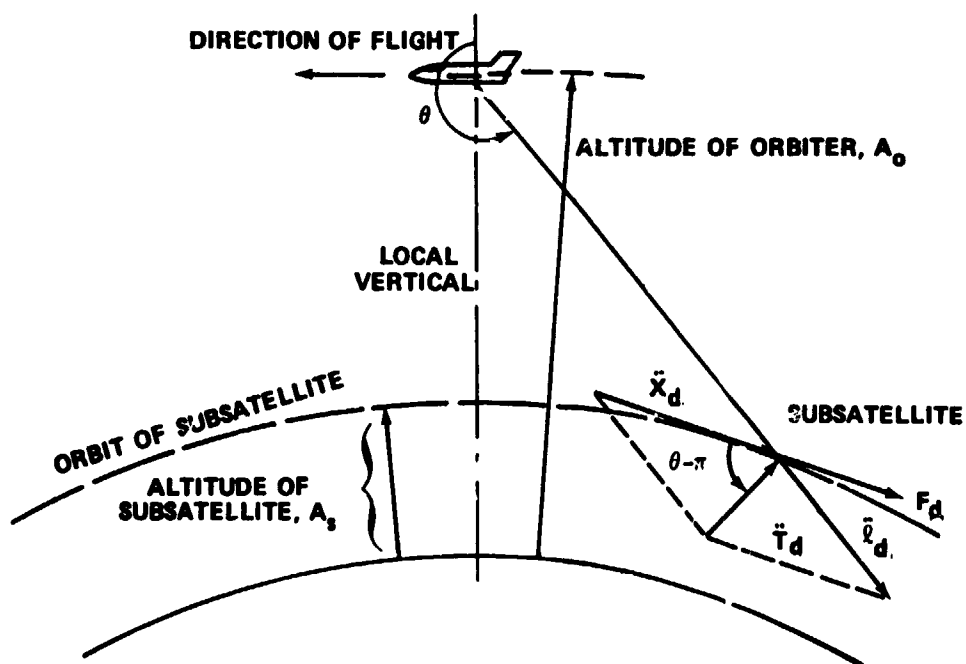$\dot{\theta}_o$ = 0.0

Figure 9. Tetherline retrieval.

23

Figure 10. Aerodynamic model of tetherline system.
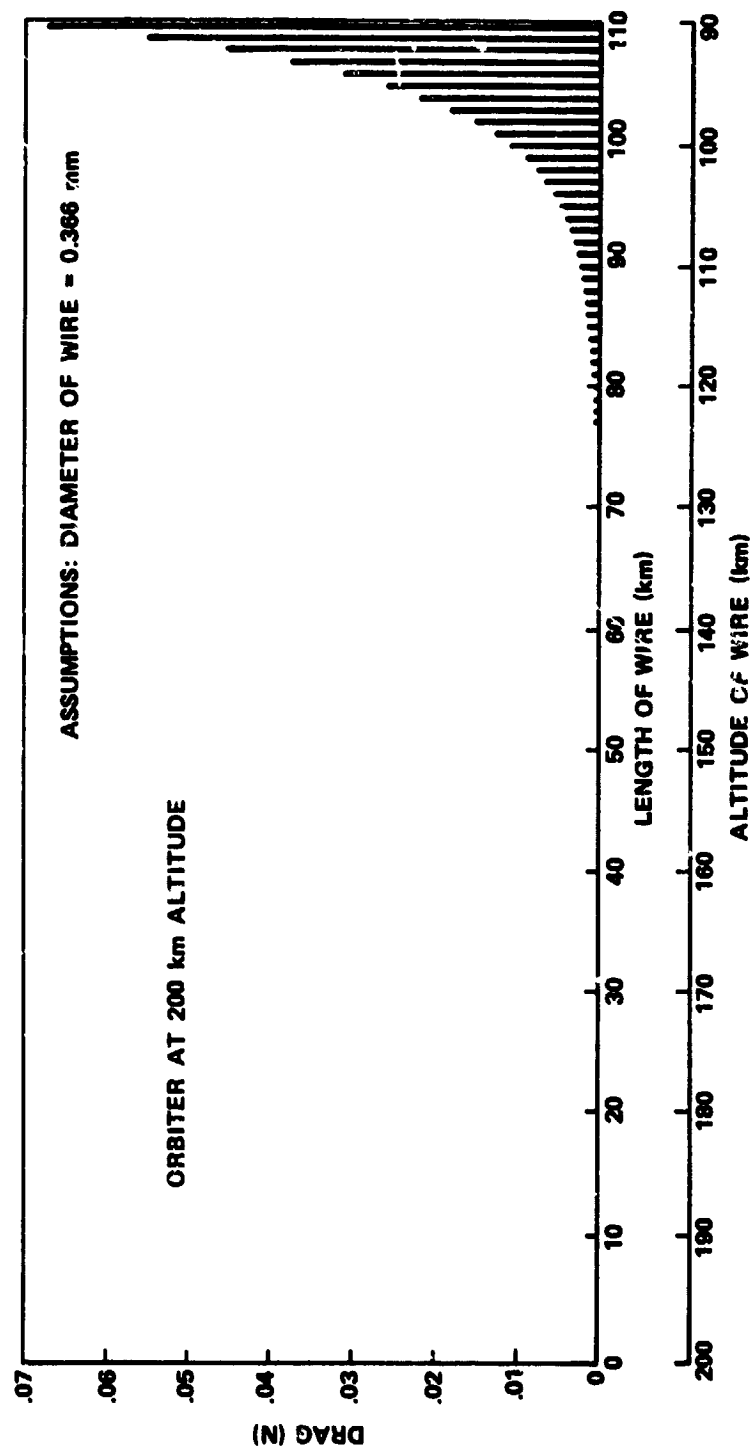
Figure 11. Aerodynamic drag on each kilometer of tetherline versus altitude.

MODIFIED TETHER CONTROL LAW: $\tau = 7 \, \dot{\phi}^2 \ell + 20 \, \dot{\phi} \, \dot{\ell} - 4 \, \dot{\phi}^2 \ell_c$

THIS PARAMETER WAS CHANGED.
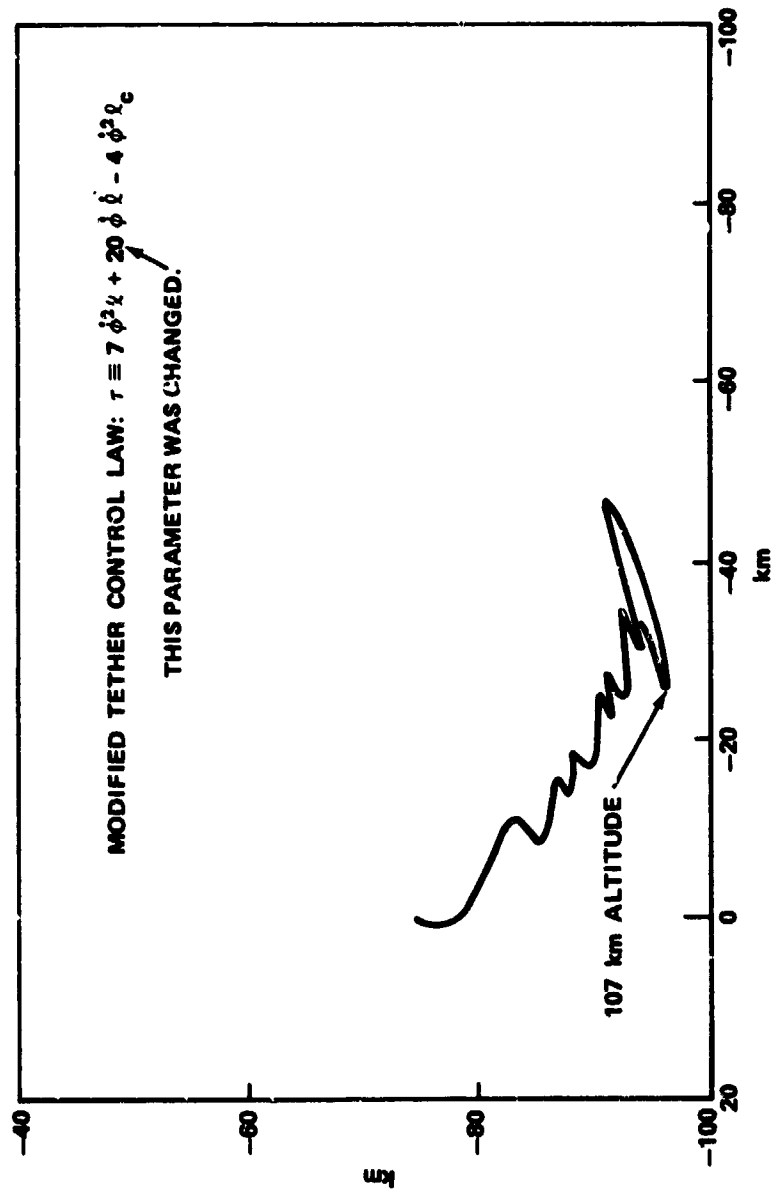
107 km ALTITUDE

Figure 12. Trajectory with atmospheric drag.

REFERENCES

1. Eades, J. B. and Wolf, Henry: Tethered Body Problems and Relative
   Motion Orbit Determination, Final Report. Contract NAS5-21453,
   Analytical Mechanics Associates, Inc., August 1972.

2. Straly, W. H. and Adlhoch, R. W.: Study of the Retrieval of an Astronaut
   from an Extra-Vehicular Assignment. The Marquardt Corp., Van Nuys,
   CA, TMC Report No. S-356, November 1, 1963.

3. Mattingly, G. S.: Presentation to Marshall Space Flight Center on
   Tethered Shuttle Payload Study Status for Langley Research Center
   by Miller Research Corp., Baltimore, MD, September 11, 1974.

4. Perrine, B. S.: A Method of Soft Tether Stationkeeping. NASA TM
   X-53643, Marshall Space Flight Center, July 31, 1967.

5. Lang, D. L. and Nolting, R. K.: Operations with Tethered Space
   Vehicles. NASA SP-138, Gemini Summary Conference, 1967.

6. Blanchard, D. L.: Dynamical Performance to Date of RAE-A (Explorer
   38). NASA TM X-63685, Marshall Space Flight Center, May 1969.

7. Colombo, E. M., et al.: Shuttle-Borne "Skyhook": A New Tool for
   Low-Orbital-Altitude Research. Proposal by Smithsonian Institution
   Astrophysical Observatory, September 1974.

APPROVAL

A TETHER TENSION CONTROL LAW FOR TETHERED SUBSATELLITES DEPLOYED ALONG LOCAL VERTICAL

By Charles C. Rupp

The information in this report has been reviewed for security classification. Review of any information concerning Department of Defense or Atomic Energy Commission programs has been made by the MSFC Security Classification Officer. This report, in its entirety, has been determined to be unclassified.

This document has also been reviewed and approved for technical accuracy.

WILLIAM R. MARSHALL
Director, Preliminary Design Office

JAMES T. MURPHY
Director, Program Development